Ursidae: The Undergraduate Research Journal at the University of Northern Colorado

Volume 6
Number 2 *McNair Special Issue*

Article 4

April 2019

Kinetic Study of Silver Nanoparticle Formation

Steven A. Diaz
University of Northern Colorado, diaz4471@bears.unco.edu

Kinetic Study of Silver Nanoparticle Formation

Steven A. Diaz
Mentor: Murielle Watzky, Ph.D., Chemistry and Biochemistry

Abstract: With the increased use of silver nanoparticles in modern day applications, kinetic information on the mechanism of their formation is useful for further studies on its reactivity in a biological environment. Silver nanoparticles were synthesized using a modified Turkevich method. The synthesized nanoparticles were characterized using UV-Visible spectroscopy. The data obtained were plotted as a function of time, and rate constants for the nucleation (k_1) and autocatalytic surface growth (k_2) were extracted. Comparing the k_1 ($\sim 10^{-3}$) and k_2 ($\sim 10^{-1}$) values supports a two-step mechanism of *slow* nucleation and *fast* autocatalytic surface growth.

Keywords: *silver nanoparticles, Turkevich method, kinetics, mechanism*

Nanoparticles (or nanoclusters) are clusters of hundreds or thousands of atoms bound together. Although its size can very, the diameter of a nanoparticle lies in the nanometer (one-billionth of a meter) range. Because of its size, metal nanoparticles have unique optical, electrical, and magnetic properties. Size causes these properties to differ from their ionic or bulk metal counterparts, which allows for the nanoparticles to be used in an array of modern technologies,[1] such as spectroscopic enhancers and antimicrobial agents as discussed below.

Silver metal nanoparticles in particular are being thoroughly studied because of their interesting physicochemical properties. Silver nanoparticles display unique optical activity caused by Localized Surface Plasmon Resonance (LSPR), which is a phenomenon occurring via the resonance of surface electrons on the nanoparticle with incoming light.[2] LSPR can be observed through absorption spectroscopy, where a broad absorption band for silver nanoparticles occurs in the ultraviolet-visible (UV-Vis) region of the electromagnetic spectrum. Furthermore, because of its strong absorption of light, silver nanoparticles possess a large extinction coefficient that can be upwards of 10^6 times larger than those of molecular chromophores[2] and is the largest among the noble metals.[3]

The unique optical properties of silver nanoparticles can be further utilized by modern spectroscopy. The LSPR of silver nanoparticles causes an electromagnetic field enhancement that in turn enhances Raman scattering of nearby molecules.[4] This property led to the development of Surface-Enhanced Raman Spectroscopy (SERS) with molecules adsorbed to the surface of silver nanoparticles.

Silver nanoparticles have also shown wide antimicrobial properties and have thus found use in antimicrobial protection thus has been integrated in many consumer products.[1] It is believed that silver atoms on the surface of nanoparticles can interact with cells upon oxidation, which releases silver(I) ions (Ag^+) that can in turn interact with multiple proteins.[3] This is particularly detrimental to bacteria, which allows silver nanoparticles to be used as antibacterial agents.

Silver nanoparticles have thus found uses in many consumer-based products because of their physicochemical and antimicrobial properties. According to the 2013 Nanotechnology Consumer Products Inventory, 435 or 24% of all nanotechnology products reported contained silver nanoparticles, making it the most frequently used nanomaterial.[1]

With their increased use, silver nanoparticle studies have also become prevalent. Most studies focus on certain aspects of the nanoparticles such as size,[4] shape,[5,6] and associated stabilizer[7,8,9], and the effect these have on the nanoparticles properties. However, these studies tend to correlate the antimicrobial attributes listed above with the activity of the nanoparticles, but most do not attempt to explain the activity “at the

molecular level."[10] Thus, there is a need to study the chemical activity of silver nanoparticles, where kinetic and mechanistic studies will attempt to provide an understanding, not just a correlation, of the mechanisms of chemical activity.

As a precursor to studies of surface reactivity of silver nanoparticles, a study of the kinetics of formation of these nanoparticles, which involved an auto-catalyzed surface growth, was performed. Kinetic information obtained through the synthesis of silver nanoparticles can thus provide key details about silver nanoparticles and the reagents (reductant and surfactant) used to make them, which in turn should provide key information on the reactivity of these silver nanoparticles. Thus, this study is intended to augment future studies by providing support of a two-step mechanism previously proposed in literature.[11]

METHODS

Materials

Silver nitrate (99%-Ag) was obtained from Strem Chemicals, Inc. and sodium citrate tribasic dihydrate (ACS reagent, ≥ 99.0%) was obtained from Sigma-Aldrich. Both reagents were used without further purification. Nanopure water was obtained using a Millipore water purification system and was collected daily to ensure the quality of the water.

Reduction of Silver Ions with Sodium Citrate

The reduction of silver nitrate to form silver nanoparticles was performed using a modified Turkevich method.[11] Silver nitrate was weighed out to the nearest milligram and dissolved in 200 mL of nanopure water. The concentration of silver nitrate was varied from $1.0x10^{-2}$ mol·L^{-1} to $1.0x10^{-4}$ mol·L^{-1}. The silver nitrate solution was mixed and brought to a boil. Once boiling, a solution of sodium citrate tribasic dihydrate was added. The concentration of sodium citrate tribasic dihydrate was varied between $1.0x10^{-2}$ to $1.0x10^{-4}$ mol·L^{-1} as well. The reaction mixture was kept at boiling temperature until the reaction had reached completion. Once the reagents had been mixed, samples of the mixture were taken for UV-Visible (UV-Vis) spectroscopic measurements.

For the UV-Vis spectroscopy measurements, the samples were taken approximately once every five minutes and cooled for one minute using an ice bath. One mL of the mixed solution was diluted with 2 mL of nanopure water in a quartz UV-Vis cell. The data were taken on an Olis® HP 8452 Diode Array and exported to Excel. The spectra were then transposed from "Absorbance vs wavelength" to "Absorbance vs time" using the reaction time measurements taken for each spectrum.

Using the Absorbance vs time graphs, rate constants were extracted using OriginLab software. The Absorbance vs time data were imported into OriginLab, where it was then used for curve-fitting. The curve-fits were performed using an integrated rate law from the literature,[12] which is described in more detail in the Results and Discussion section.

RESULTS AND DISCUSSION

Multiple spectra of a synthesis were taken at varying times. A wavelength of 414 nm typically resulted in large absorbance values, as can be seen in Figure 1. The collection of a series of spectra allowed for the formation of silver nanoparticles to be followed as a function of time.

Using a wavelength of 414 nm, plots of absorbance versus time were created (Figure 2). These plots were then exported into OriginLab to extract kinetic rate constants through nonlinear curve fitting (Figure 3). Nonlinear curve-fits were calculated using an integrated rate law as previously published in the literature.[12]

Figure 1. A series of spectra obtained during a synthesis of silver nanoparticles using 1.00×10^{-3} mol·L^{-1} silver nitrate and 9.86×10^{-4} mol·L^{-1} sodium citrate tribasic dihydrate.

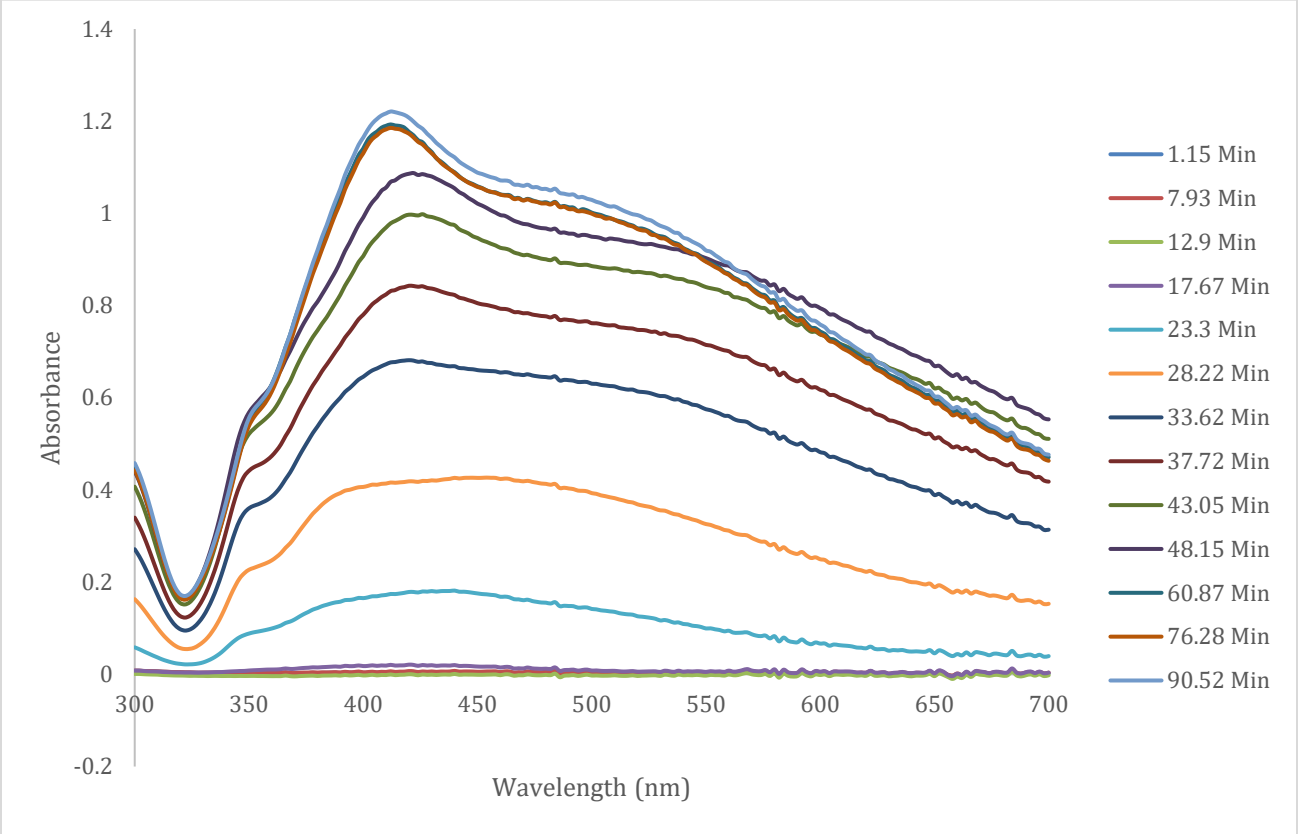

The integrated rate law published in the literature[12] corresponds to a two-step mechanism of silver nanoparticle formation that consists of a slow nucleation and a fast autocatalytic surface growth. In the first step, the silver(I) ions ("A") are reduced to silver(0) metal and aggregate to form a cluster of critical size ("B") (Equation 1). Once the cluster of critical size is formed, it catalyzes the reduction of silver(I) ions to silver(0) metal on its surface (Equation 2). The integrated raw law for this process (Equation 3) was used to curve fit the data obtained via UV-Vis spectroscopy, which allowed for the extraction of the rate constants k_1 and k_2 for nucleation and growth, respectively.

$$A \xrightarrow{k_1} B \quad (1)$$

$$A + B \xrightarrow{k_2} 2B \quad (2)$$

$$[B]_t = [A]_0 - \frac{\frac{k_1}{k_2} + [A]_0}{1 + \frac{k_1}{k_2[A]_0} \cdot e^{(k_1 + k_2[A]_0)t}} \quad (3)$$

The rate constants for syntheses using a 1 to 1 molar ratio 1.0×10^{-3} mol·L^{-1} of silver nitrate to 1.0×10^{-3} mol·L^{-1} sodium citrate were tabulated along with their corresponding absorbance values, standard deviations, and R^2 values (Table 1). The curve-fits show good R^2 values for each plot, which indicates a good fit to the two-step mechanism of nucleation and autocatalytic surface growth for the formation of silver nanoparticles. Also, the rate constants for nucleation (k_1) and autocatalytic surface growth (k_2) are found to differ by approximately three orders of magnitude (Table 1), which again supports the two-step mechanism. The large standard deviations in the

nucleation rate constant (k_1) show that only the magnitude of the rate constant is known; however, this can be attributed to the limited amount of absorbance data points taken between 0 and 20 minutes. As such, more syntheses and absorbance data points prior to the 20-minute mark are required.

The reproducibility of the syntheses was confirmed using the data in Table 1. When comparing the average k_1 and k_2 values and their standard deviation, the k_1 and k_2 values fall within the average and standard deviation. This means that the data taken are equivalent within error. As such, the data taken was reproducible.

Figure 2. A transposed plot of time vs absorbance at 414 nm of a silver nanoparticle synthesis using $1.00x10^{-3}$ mol·L^{-1} silver nitrate and $9.86x10^{-4}$ mol·L^{-1} sodium citrate tribasic dihydrate.

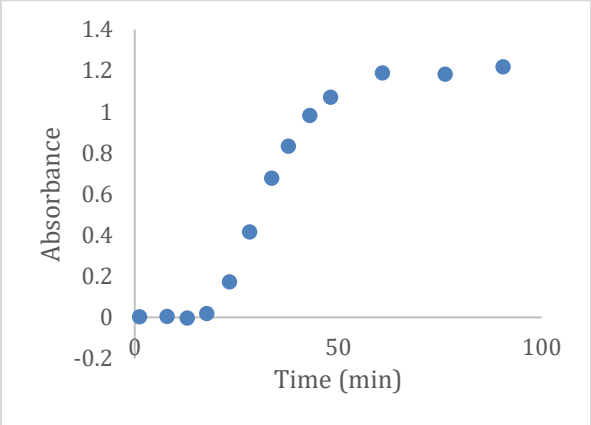

Figure 3. A curve-fitted plot made using the data set from Figure 2.

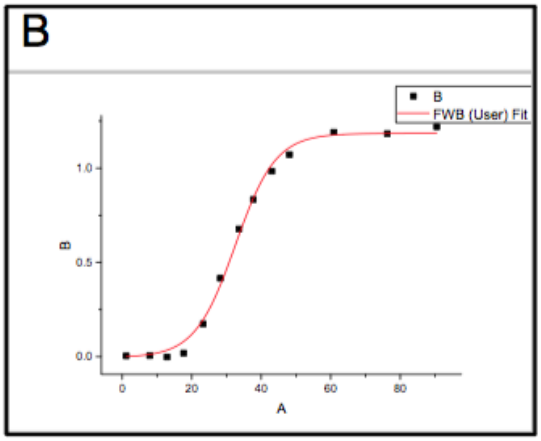

Table 1. Nucleation rate constants (k_1) and autocatalytic surface growth (k_2) for $1.0x10^{-3}$ mol·L^{-1} silver nitrate and $1.0x10^{-3}$ mol·L^{-1} sodium citrate reactions as extracted using OriginLab software.

Synthesis	Maximum Absorbance[a]	k_1 (min^{-1})	k_2 (ABS^{-1}min^{-1})[b]	R^2
1	1.368±0.023	(3.25±1.65) x10^{-4}	0.173±0.018	0.998
2	1.195±0.023	(1.08±0.41) x10^{-3}	0.146±0.016	0.995
3	0.861±0.026	(1.53±0.48) x10^{-3}	0.124±0.016	0.990
4	1.185±0.019	(6.31±2.07) x10^{-4}	0.145±0.012	0.995
Average	1.152±0.213	(8.92±5.27) x10^{-4}	0.147±0.020	

[a]Absorbance is a unit-less quantity.
[b]ABS stands for absorbance units, which is a unit-less quantity.

Syntheses with different initial concentrations of silver nitrate and sodium citrate were also performed. Rate constants for these syntheses were tabulated, along with their maximum absorbance values using a wavelength of 414 nm, their standard deviations, and R^2 values (Table 2).

By changing the concentrations of silver nitrate, sodium citrate, and the ratio between the two, it was found that the maximum absorbance and rate constants (k_1 and k_2) were affected. For example, as the sodium citrate concentration is decreased, the maximum absorbance, which is directly related to the concentration of silver nanoparticles, is also decreased (see syntheses 2-5 at constant initial silver nitrate concentration). This can be explained by the fact that there was not enough citrate to reduce silver(I) ions to silver(0) metal. Similarly, the k_1 values also decreased (see syntheses 2-5 at constant initial silver nitrate concentration). Again, this can be explained by the diminished presence of sodium citrate, which had the effect of slowing down the initial reduction of silver(I) ions to silver(0) metal. On the other hand, the k_2 values displayed a small increase when the sodium citrate concentration

was decreased (see syntheses 2-5 at constant initial silver nitrate concentration). This can be explained by the fact that these account for the (autocatalyzed) reduction of silver(I) ions to silver(0) metal *at the nanocluster surface*, so that having less sodium citrate, which is also the stabilizer for these nanoparticles, leaves more room on the nanocluster surface.

As this study was intended to increase current information on silver nanoparticle formation, some limitations were encountered. It should be noted that more experiments in which the sodium citrate concentration is *increased* with respect to the silver nitrate concentration will be needed in order to determine any trend in maximum absorbance and rate constants (k_1 and k_2). Also, it was also found that deviating from $1.0x10^{-3}$ $mol \cdot L^{-1}$ silver nitrate and $1.0x10^{-3}$ $mol \cdot L^{-1}$ sodium citrate concentrations could cause syntheses to behave non-ideally. For example, a reaction using a 1 to 1 ratio of silver nitrate to sodium citrate, but with concentrations of $1.0x10^{-2}$ $mol \cdot L^{-1}$ for both reagents, was performed. There, the concentrations of both starting reagents was found to be sufficiently high for a thin silver film to form on the reaction flask. In conclusion, the findings of this study could provide a starting ground for future studies regarding silver nanoparticle kinetics.

Conclusion

Silver nanoparticles were synthesized using the Turkevich method. The syntheses were then characterized using UV-Vis spectroscopy. Using the data obtained, plots of Absorbance vs time were created to extract kinetic rate constants from nonlinear curve-fits. Nonlinear curve-fits were performed in OriginLab, using an integrated rate law for a two-step mechanism of nucleation and growth. The syntheses were found to be reproducible, and rate constants were determined using multiple syntheses. The rate constants for nucleation and growth were found to differ by approximately three orders of magnitudes, which supports a two-step mechanism of *slow* nucleation and *fast* autocatalytic surface growth. Although limitations of the study included limited data on increased reagent starting conditions, future studies addressing the limitations could further augment the conclusion stated above.

Table 2. Nucleation rate constants (k_1) and autocatalytic surface growth (k_2) for silver nanoparticle formation using different initial molar concentrations of silver nitrate and sodium citrate.

Synthesis	$[AgNO_3]$ $x10^3$ ($mol \cdot L^{-1}$)	$[Na_3Cit]^c$ $x10^3$ ($mol \cdot L^{-1}$)	Ratio of Cit^d/Ag^+	Maximum Absorbance[e]	k_1 (min^{-1})	k_2 ($ABS^{-1}min^{-1}$)	R^2
1[f]	N/A	N/A	N/A	1.152±0.213	(8.92±5.27) $x10^{-4}$	0.147±0.020	N/A
2	0.985	0.511	0.519	1.20±0.02	(3.73±0.71) $x10^{-4}$	0.113±0.006	0.997
3	1.01	0.200	0.198	0.760±0.012	(2.34±0.51) $x10^{-4}$	0.181±0.010	0.995
4	1.00	0.0975	0.0975	0.344±0.015	(7.41±8.29) $x10^{-5}$	0.480±0.098	0.947
5	1.03	0.0936	0.0909	0.380±0.012	(8.41±3.78) $x10^{-5}$	0.276±0.029	0.981
6	0.198	1.05	5.30	0.295±0.002	(5.86±0.90) $x10^{-5}$	0.428±0.013	0.999

[c]Sodium citrate tribasic dihydrate is abbreviated as Na_3Cit.
[d]Citrate ion is abbreviated as Cit.
[e]Maximum absorbance pulled from curve-fits.
[f]Synthesis 1 is the average of a 1 to 1 ratio of sodium citrate to silver nitrate as calculated for Table 1.

REFERENCES

1. Vance, M. E.; Kuiken, T.; Vejerano, E. P.; McGinnis, S. P.; Hochella Jr., M. F.; Rejeski, D.; Hull, M. S. *Beilstein J. Nanotechnol.* **2015**, *6*, 1769-1780.
2. Campbell, D. J.; Xia, Y. *J. Chem. Educ.* **2007**, *84*, 91-96.
3. Krutyakov, Y. A.; Kudrinskiy, A. A.; Olenin, A. Y.; Lisichkin, G. V. *Russian Chemical Review.* **2008**, *77*, 233-257.
4. Stamplecoskie, K. G.; Scaiano, J. C.; Tiwari, V.; Anis, H. *J. Phys. Chem. C.* **2011**, *115*, 1403-1409.
5. Dong, X.; Ji, X.; Jing, J.; Li, M.; Yang, W. *J. Phys. Chem. C.* **2010**, *114*, 2070-2074.
6. Ringe, E.; Zhang, J.; Langille, M. R.; Sohn, K.; Cobley, C.; Au, L.; Xia, Y.; Mirkin, C. A.; Huang, J.; Marks, L. D.; Van Duyne, R. P., *Mater. Res. Soc. Symp. Proc.* **2009**, *1208.*
7. El Badawy, A. M.; Silva, R. G.; Morris, B.; Scheckel, K. G.; Suidan, M. T.; Tolaymat, T. M. *Environ. Sci. Technol.* **2011**, *45*, 283-287.
8. Kvítek, L.; Panáček, A.; Soukupová, J.; Kolář, M.; Večeřová, R.; Prucek, R.; Holecová, M.; Zbořil, R. *J. Phys. Chem. C.* **2008**, *112,* 5825-5834.
9. Pillai, Z. S.; Kamat, P. V. *J. Phys. Chem. B.* **2004**, *108*, 945-941.
10. Murphy, C. J.; Vartanian, A. M.; Geiger, F. M.; Hamers, R. J.; Pedersen, J.; Cui, Q.; Haynes, C. L.; Carlson, E. E.; Hernandez, R.; Klaper, R. D.; Orr, G.; Rosenzweig, Z. *ACS Cent. Sci.*, **2015** *1*, 117-123.
11. Turkevich, J.; Stevenson, P. C.; Hiller, J. *Discuss. Faraday Soc.* **1951**, *11*, 55-75.
12. Watzky, M. A.; Finke, R. G. *J. Am. Chem. Soc.* **1997**, *119*, 10382-10400.